Structure and Biological Activity of a Host-Specific Toxin Produced by the Fungal Corn Pathogen *Phyllosticta maydis*†

Stephen J. Danko, Y. Kono, J. M. Daly,* Yoshikatsu Suzuki, S. Takeuchi, and David A. McCrery

ABSTRACT: A host-specific pathotoxin affecting susceptible corn (*Zea mays*) with Texas male sterile cytoplasm has been isolated from cultures of the corn pathogen *Phyllosticta maydis*. The toxin (PM toxin) consists of 10–15 components, of which the four major ones are shown to be linear C_{33} and C_{35} compounds containing β-keto alcohol functional groups. The positions of the functional groups have been deduced by nuclear magnetic resonance spectroscopy of acetate derivatives and by mass spectroscopy of trimethylsilyl and phenylboronate derivatives. PM toxin has no effect on resistant corn at 10^{-5} M, but each purified component of PM toxin has the same high toxicity (10^{-8}–10^{-9} M) toward tissues and mitochondria obtained from susceptible corn varieties as does HMT toxin previously isolated from the unrelated plant pathogen *Helminthosporium maydis*. The similarities in structure between these unusual, highly selective toxicants may be useful in elucidating their modes of action.

A number of fungal plant pathogens, particularly members of the genera *Helminthosporium* and *Alternaria*, produce host-selective or -specific pathotoxins that are important determinants of plant disease in susceptible hosts. Studies on the biochemical basis of their marked specificity for, and high toxicity toward, susceptible host plants has been limited because their chemical nature was unknown. Very recent research has shown that host-selective pathotoxins comprise a diverse array of chemical structures [reviewed by Kono et al. (1981) and Daly et al. (1983)], even when produced by species of the same genera.

Helminthosporium maydis, race T, the cause of major epidemics of Southern corn leaf blight of corn, produces a pathotoxin consisting of a series of 8–10 unusual linear β-polyketols with an odd number of carbon atoms (C_{35}–C_{45}) (Kono & Daly, 1979; Kono et al., 1980). Each component exhibits equal and high toxicity (10^{-8}–10^{-9} M) toward susceptible corn carrying Texas male sterile (Tms) cytoplasm, but none have effects on corn with normal (N) cytoplasm at 10^{-6}–10^{-5} M (Payne et al., 1980a). The four major components, C_{39} and C_{41}, comprising 70-90% of the native toxin (HMT toxin), are shown in Figure 1. The chemically unrelated insecticide methomyl [$CH_3C(SCH_3)$=N—O—C(O)—NH_2—CH_3] also selectively damages Tms corn but at much higher concentrations (10^{-2}–10^{-3} M) (Koeppe et al., 1978) than HMT toxin.

Two independent reports (Yoder, 1973; Comstock et al., 1973) indicate that the taxonomically unrelated corn pathogen *Phyllosticta maydis*, cause of a destructive leaf blight occurring during the spring in the northern U.S., also produces a toxin (PM toxin) with the same specificity toward Tms corn as HMT toxin from *H. maydis*. However, it was not established if PM toxin was chemically related to either HMT toxin or methomyl. In this paper, we describe the identification of several toxin species from *P. maydis* that have the same high toxicity toward Tms corn as HMT toxin from *H. maydis*. The evidence to be presented indicates that the structures of PM toxins (Figure 2) are different from those of HMT toxin, but they have certain similarities that may be useful in investigating their biochemical mode of action. In addition to intrinsic importance for understanding plant disease resistance, determination of the mode of action of these toxicants has theoretical and practical implications for our understanding of the biochemistry of genetic sterility in higher plants (Leaver & Gray, 1982).

Materials and Methods

Toxin Isolation and Purification. The procedures were similar to those used for HMT toxin from *Helminthosporium maydis* (Kono & Daly, 1979; Tegtmeier et al., 1982). *Phyllosticta maydis* was grown for 15 days on modified Fries medium (Pringle & Scheffer, 1963) in still liquid culture at 20–21 °C under continuous fluorescent light (50 $\mu E \cdot m^{-2} \cdot s^{-1}$). Mycelium was removed by filtration through Miracloth (Calbiochem) and the toxin removed from the culture fluids by adsorption onto Norit A (3%, w/v). Mycelium was blended with 70:30 acetone–water 3 times for 10 min each in a Waring Blendor. The acetone–water filtrate then was treated with the same batch of Norit A used to extract toxin from culture filtrates.

After adsorption of toxin, the Norit A was rinsed well with 70:30 acetone–water and then with neat acetone. Toxin was extracted by three 1-h treatments with 500 mL of chloroform–methanol (95:5), which were combined, filtered, and reduced to dryness in vacuo at 45–50 °C. The residue was dissolved in approximately 50 mL of warm chloroform and passed through a fine sintered-glass filter to remove particulates. After being allowed to dry, the residue was dissolved in 5–10 mL of warm acetone and placed at −10 °C overnight. The resulting white precipitate was reprecipitated at room temperature from acetone, chloroform, or methanol. Individual components were separated by thin-layer chromatography (TLC) on Merck EM 60 silica gel plates with chloroform–methanol (85:15). They were extracted from the silica gel with several volumes of warm acetone and centrifuged to remove particulates before being dried under a stream of nitrogen. Each component then was precipitated twice from acetone at −10 °C. The activity of PM toxin was measured either by inhibition of dark CO_2 fixation of thin leaf slices of susceptible (inbred line W64AT) corn (Daly & Barna, 1980) or by effects on mitochondrial oxidation (Suzuki et al., 1983).

† From the Departments of Agricultural Biochemistry (S.J.D. and J.M.D.) and Chemistry (D.A.M.), University of Nebraska, Lincoln, Nebraska 68583-0718, and the Institute of Physical and Chemical Research, Wako-shi, Saitama 351, Japan (Y.K., Y.S., and S.T.). *Received July 5, 1983.* This is Paper No. 7213 from the Nebraska Agricultural Experiment Station. This work was partially supported by USDA CRGO Grant 82-CRCR-1-1096, NSF Grant PCM-79 20685, and a Grant-in-Aid for Scientific Research from the Japan Ministry of Education, Science and Culture.

0006-2960/84/0423-0759$01.50/0

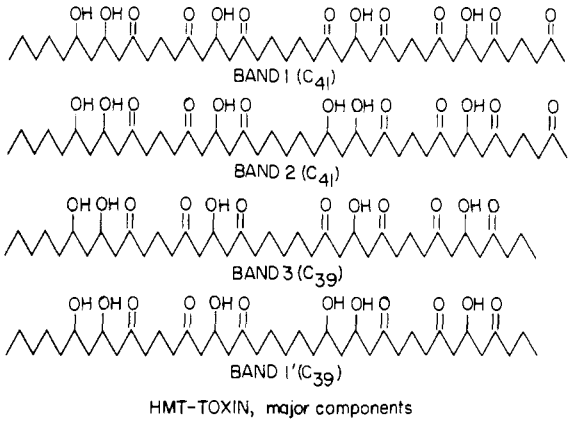

FIGURE 1: Structures of major components (designated as bands) of host-specific HMT toxin produced by *H. maydis* and affecting only corn with Texas male sterile cytoplasm. Each component is equally active at $\simeq 10^{-9}$ M on physiological processes of susceptible corn.

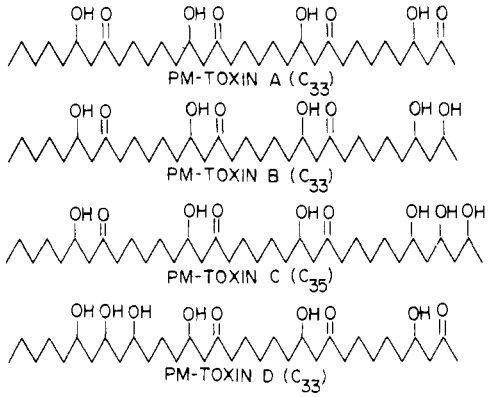

FIGURE 2: Summary of postulated structures for the four main toxic components obtained from the fungal corn pathogen *P. maydis*.

Preparation of Derivatives. Acetylation of isolated components was accomplished by dissolving approximately 1–2 mg in 0.5 mL of pyridine (dried over KOH) and adding 0.3 mL of acetic anhydride at 4 °C. After concentration under vacuum, the residue was dissolved in dichloromethane–2-propanol (98.5:1.5) and subjected to high-performance liquid chromatography (HPLC) on Nucleosil (Macherey-Nagel, 5 μm). Absorption at 280 nm revealed a major (80%) and a few minor peaks arising from incomplete acetylation or degradation. The main peak was rechromatographed twice.

Hydrocarbons were prepared by adaptation of the methods of Cope et al. (1962). One to two milligrams of toxin acetate was reduced with Adams catalyst (20–30 mg) in methanol–acetic acid (9:1, 10 mL) for 72–96 h until ^{1}H NMR (proton nuclear magnetic resonance) of active methylene groups indicated the keto groups had been reduced. After removal of catalyst and solvent evaporation, the oily residue was heated with red phosphorus (20 mg) under reflux for 24 h in excess constant-boiling hydriodic acid (3 mL) and *n*-heptane (2 mL). Water (5–10 mL) was added to the mixture, followed by extraction with chloroform (10 mL) 3 times. The combined extracts were washed with 2% sodium thiosulfate solution (1 mL) and then with water (3 mL, 3 times) and dried over magnesium sulfate. Removal of solvent gave an iodine-containing oil that was dissolved in tetrahydrofuran (3–5 mL) and refluxed overnight with lithium aluminium hydride (10–20 mg). Workup was accomplished by successive addition of water (10–20 μL), 15% sodium hydroxide solution (10–20 μL), and water (30–60 μL). The precipitate was washed with chloroform (10 mL). Then, the residual tetrahydrofuran and chloroform solutions were combined, and after evaporation of the solvents, the residue was rehalogenated by the above method (red phosphorus and hydriodic acid) without *n*-heptane. This product was dehalogenated with lithium aluminum hydride as above. The product was hydrogenated with Adams catalyst (10 mg) in *n*-hexane and ethyl acetate (2:1, 10 mL) for 1 h. After removal of catalyst, the solvent was evaporated, and products were separated by silica gel (Merck Kieselgel 60, 230–240 mesh) column chromatography with *n*-hexane. The eluate was analyzed by GC–MS (gas chromatography–mass spectroscopy).

Table I: Percentage Inhibition by Native PM and HMT Toxins of Dark CO_2 Fixation in Leaf Slices of Susceptible (W64AT) Corn[a]

	percentage inhibition at a concentration (ng/mL) of				
compound	1	3	10	30	100
native HMT toxin	4 ± 2	4 ± 9	14 ± 2	21 ± 2	44 ± 1
native PM toxin	13 ± 1	22 ± 2	30 ± 3	44 ± 1	51 ± 2

[a] Average of two experiments with three replicates each, 15 leaf slices per replicate. Control rate 21.7 ± 0.1 μmol of $^{14}CO_2$ fixed h^{-1} $slice^{-1}$.

For the preparation of silyl ethers, toxins (100–200 μg) were dissolved in dry pyridine (0.5 mL), and 0.1 mL of hexamethyldisilazane and 0.05 mL of trimethylchlorosilane were added at 0 °C. After 1 h, the reaction mixture was concentrated in vacuo. The product was dissolved in CCl_4 (0.1 mL) and analyzed by EI-MS (electron-impact mass spectroscopy).

Preparation of phenylboronate esters was accomplished by dissolving 200–300 μg of toxin in dry pyridine (0.3 mL), and phenylboronic acid (2 mg) in dry pyridine (0.1 mL) was added at 0 °C. The products were silylated by adding, after 2 h, 0.1 mL of hexamethyldisilazane and 0.05 mL of trimethylchlorosilane. The product was analyzed as above.

Toxins also were derivatized after reduction of carbonyl groups. Toxins (100–200 μg) were dissolved in MeOH (0.5 mL), and $NaBH_4$ (2 mg) or $NaBD_4$ (2 mg) was added at 0 °C. After 30 min, 0.1 mL of acetic acid was added, and the reaction mixture was concentrated in vacuo. The product was treated with phenylboronic acid and hexamethyldisilane and analyzed as above.

GC analysis was performed with a Shimadzu GC-4B (OV-1, 4 mm × 50 mm column). Spectra were obtained with the following instruments: low-resolution MS, Hitachi RMU-6MG; high-resolution MS, Hitachi M-80 or Kratos MS-50; FAB-MS, Kratos MS-50; ^{1}H NMR, Jeol Fx-400 or Gx-400 (400 MHz) or Nicolet NT 360 (360 MHz); ^{13}C NMR, Jeol Fx-90 Q (22.5 MHz); IR, Shimadzu IR-435.

Results and Discussion

Isolation and Biological Activity of PM Toxin. PM toxin was produced in amounts sufficient for isolation as a white powder after 15 days of still culture but only at temperatures of 20–22 °C and under light. When *P. maydis* was grown at higher temperatures or in darkness, small, unrecoverable amounts of toxin could be detected by bioassay but only after longer periods of growth. Yields were somewhat variable but typically represented 0.25% of the mycelial dry weight, with culture fluids accounting for less than 15% and homogenized mycelium for over 85% of the final yield. The yield on a mycelial weight basis is much less than that for HMT toxin ($\simeq$3%), and in addition, mycelial growth of *P. maydis* also is appreciably less under these conditions.

Table I compares the inhibitory effects of HMT and PM toxins on dark CO_2 fixation by leaf slices of susceptible

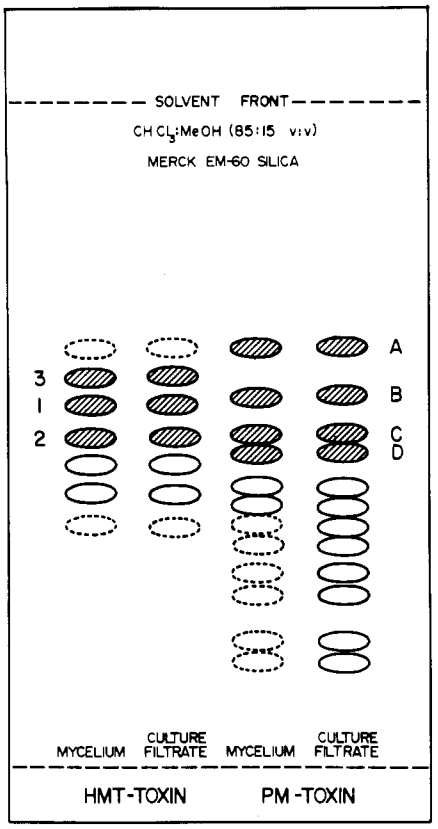

FIGURE 3: Patterns of HMT and PM toxins on commercial Merck EM 60 TLC plates with $CHCl_3$–MeOH (85:15), stained with I_2. Shaded areas give the most intense stain; clear areas are of moderate stain; dotted areas are faint stains. Individual channels are of toxin obtained separately from mycelium or culture filtrates. Culture filtrates from *P. maydis* are relatively enriched in more hydrophilic components, but the total yield of toxin is much greater from mycelium.

(W64AT) corn. On a weight basis, native PM toxin is somewhat more inhibitory than HMT toxin. There was no inhibition of dark CO_2 fixation in leaf slices of resistant (W64AN) corn at concentrations as high as 10 μg/mL.

A TLC comparison of PM and HMT toxins showed that, although their R_f values in chloroform–methanol (85:15) are similar, the pattern for the individual components of each toxin is distinctive (Figure 3). *P. maydis* culture fluids were enriched in the more hydrophilic components with lower R_f values, but these same components could also be detected in mycelium if the TLC plates were overloaded with sample.

When stained with iodine vapors, PM toxins A–D appeared to constitute 70–80% of the materials on the plates. The observations were supported by the fact that, per 100 mg of white precipitate applied to 60 plates, 6.1, 10.0, and 8.7 mg, respectively, were recovered for PM toxins A–C in pure form, while only 11.4 mg was recovered for all other components including PM toxin D. The low yields resulted from ready conversion to yellow and red pigments during isolation.

Properties of PM Toxins. When purified, each component was a white powder. Some of the properties of the purified components are given in Table II. The IR spectra of the compounds were nearly identical and very similar to HMT toxin: ν_{max}^{KBr} 3400 (OH), 2930 and 2850 (CH_2CH_3), 1709 (C=O), 1465 and 1402 ("active" CH_2). After PM toxins B and C were reduced by the procedures of Cope et al. (1962), GC–MS revealed retention times and fragmentation patterns typical of linear alkanes. The parent ions of the hydrocarbons corresponded to $C_{33}H_{68}$ and $C_{35}H_{72}$ for toxins B and C, respectively (Table II). FD–MS of the sodium complexes and FAB-MS of free toxins yielded molecular masses of 584, 586, 630, and 602 for PM toxins A–D, respectively. On the basis of analogy with the elemental composition of HMT toxin (C, H, O), empirical formulae were calculated (Table II). From the index of hydrogen deficiency and on the basis of the presence of C=O absorption in the IR spectra, the number of carbonyl and presumed secondary alcohol groups was estimated. The estimates of hydroxyl groups were supported by the proton integration values obtained from 400-MHz spectra of the acetylated toxins in $CDCl_3$ (Table II).

The 400-MHz ^1H NMR spectra of PM toxin acetates were different in several significant features from those of HMT

Table II: Some General Chemical Properties and Proposed Functional Groups of the Four Main Components of Pathotoxin from *P. maydis*

	PM toxin			
	A	B	C	D
mp (°C)	118-119	97-98	108-109	110-111
UV spectra[a]				
λ_{max} (nm)	276	275	276	276
ϵ	195	138	130	118
$[\alpha]_D$ (deg)[a,b]	−11	−10	−6	−8
hydrocarbon				
m/z		464	492	
C_nH_{n+2}		$C_{33}H_{68}$	$C_{35}H_{72}$	
molecular ions $(M + H)^+$				
FAB-MS (free toxin)	585	587	631	603
FD-MS (Na complex)	607	609	653	625
empirical formula[c]	$C_{33}H_{60}O_8$	$C_{33}H_{62}O_8$	$C_{35}H_{66}O_9$	$C_{33}H_{62}O_9$
secondary alcohol groups[c]	4	5	6	6
carbonyl groups[c]	4	3	3	3
^1H integration of acetate[d]				
observed	69	72	79	73
expected	68	72	78	74

[a] In methanol. [b] At 25, 27, 27, and 35 °C for A–D. [c] Calculated with the assumption of only C, H, and O. [d] 400-MHz NMR spectra in $CDCl_3$.

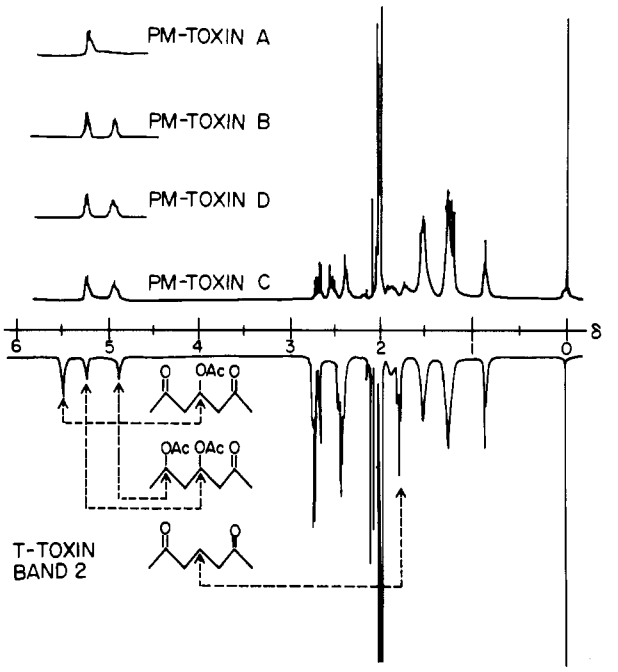

FIGURE 4: Comparison of 400-MHz proton NMR spectra of PM toxin C acetate (upper section) and HMT toxin band 2 (see Figure 1) acetate (lower section). The partial structures and dotted lines for HMT toxin band 2 toxin acetate indicate chemical-shift assignments made by Kono & Daly (1979). See text for details.

Table III: Low-Resolution Mass Spectral Data of Trimethylsilyl Ether and Phenylboronate Ester Derivatives of PM Toxins

	PM toxin			
	A	B	C	D
	(1) Me_3Si Ethers			
base peak	173	173	173	173
ref peak	577	117	117	117
M^+ (%)	872 (2)[a]	946 (0.3)	1062 (0.1)	1034 (<1)
$M^+ - CH_3$ (%)	857 (7)	931 (2)	1047 (0.2)	1019 (3)
formula	$C_{45}H_{92}O_8Si_4$	$C_{48}H_{102}O_8Si_5$	$C_{53}H_{114}O_9Si_6$	$C_{51}H_{110}O_9Si_6$
	(2) Phenylboronate Esters $\longrightarrow$ Me_3Si Ethers			
base peak	173	173	173	173
ref peak	692	511	511	491
M^+ (%)	872 (3)	888 (4)	1004 (0.5)	976 (3)
$M^+ - CH_3$ (%)	857 (15)	873 (21)	989 (13)	961 (20)
formula	$C_{45}H_{92}O_8Si_4$	$C_{48}H_{89}O_8Si_3B$	$C_{53}H_{101}O_9Si_4B$	$C_{51}H_{97}O_9Si_4B$
	(3) $NaBH_4$ $\longrightarrow$ Phenylboronate Esters			
base peak	207	161	161	
M^+	936 (42)	936 (58)	980 (<0.1)	
$M^+ - CH_3$ (%)	921 (<1)	921 (<1)	965 (<1)	
formula	$C_{57}H_{80}O_8B_4$	$C_{57}H_{80}O_8B_4$	$C_{59}H_{84}O_9B_4$	
	(4) $NaBH_4$ $\longrightarrow$ Phenylboronate Esters $\longrightarrow$ Me_3Si Ethers			
base peak	207	207	117	173
ref peak	207	207	161	161
M^+ (%)	936 (58)	936 (58)	1052 (7)	1024 (5)
$M^+ - CH_3$ (%)	921 (1)	921 (1)	1037 (7)	1009 (6)
formula	$C_{57}H_{80}O_8B_4$	$C_{57}H_{80}O_8B_4$	$C_{62}H_{92}O_9SiB_4$	$C_{60}H_{88}O_9SiB_4$

[a] Numbers in parentheses are peak intensities as a percentage of the reference peak.

toxin acetates. The differences are illustrated in Figure 4, which compares the complete spectra of PM toxin C and HMT toxin band 2 (Figure 1) acetates. The spectra of all HMT toxin acetates show signals at δ 5.48, 5.23, and 4.90 (Figure 4), which were assigned (Kono & Daly, 1979) to methine protons of secondary alcohols. The secondary alcohol groups of HMT toxin are present in either β,δ-dioxy oxo or β,β'-dioxo oxy functions (Figures 1 and 4). The absorption at δ 5.48, assigned to a methine proton flanked by two β,β'-keto groups, was absent (Figure 4) from the spectra of all PM toxin acetates. However, the latter spectra all share with HMT toxin spectra a chemical shift at δ 5.23 that integrates for three protons in PM toxins B–D and for four protons in PM toxin A. This chemical shift in HMT toxin previously was assigned to a methine proton β to a carbonyl function (Figure 4). The third signal at δ 4.90 in HMT toxin spectra (Figure 4) is shifted to approximately δ 4.94 in PM toxins B–D, integrating for two, three, and three protons, respectively. However, this absorption was absent from the spectra of PM toxin A acetate (Figure 4).

These results indicated that the β,β'-dioxo oxy function of HMT toxin (Figure 1) is absent in PM toxins. Instead, the latter toxins may have either β,δ-dioxy oxo functions (Figure 1) and/or β-oxy oxo (β-keto alcohol) groups. The latter possibility is suggested by the fact that PM toxin A has only a single signal at δ 5.23 integrating for four protons that can be assigned to protons of secondary alcohols β to carbonyl groups (Figures 1 and 4). PM toxins B–D may have three such groups, plus a β-dioxy function or β-dioxy oxo function.

In addition, a signal at approximately δ 1.80, integrating for eight protons in HMT toxin spectra, is reduced in PM toxins (Figure 4). At least four protons in this region can be ascribed to the central methylene carbon of two $-(CH_2)_3-$ bridges between oxygen functions in HMT toxins (Figure 1). From consideration of the empirical formula of PM toxin A (Table II), the methylene bridges between carbonyl functions can be longer than three methylene groups. Four β-keto alcohol functions separated by $-(CH_2)_5-$ bridges would be permissible from the data for PM toxin A (Table II).

Mass Spectra of Derivatives. Phenylboronate derivatives were stable during electron-impact mass spectrometry (EI-MS), and generally, peak intensity could be expressed as a percentage of the base peak of m/z 161 ($C_9H_{10}O_2B$). EI-MS spectra of Me_3Si ether derivatives of PM toxins yielded a very intense base peak of m/z 173 ($C_9H_{21}OSi$) and/or m/z 117 ($C_5H_{13}OSi$). Because of extensive fragmentation, as well as a lack of volatility, it was not always possible to reference the larger masses in terms of these peaks. Rather, the intensities had to be calculated as a percentage of the largest peak that could be measured at an appropriate spectrometer amplification for the larger masses.

Table III summarizes some diagnostic features in the mass spectra of four sets of derivatives. The molecular ions of Me_3Si ethers of PM toxins A–D (Table III, part 1) established four, five, six, and six hydroxyl groups, respectively, in agreement with the calculations of Table II. In addition, a characteristic sequence of ions representing successsive loss of 90 mass units (Me_3SiOH) was observed for all spectra. Formation of monophenylboronate derivatives (Table III, part 2) indicated the presence of at least one set of β-secondary alcohol groups in PM toxins B–D but not in PM toxin A since this toxin did not react with phenylboronate.

However, the parent ions obtained by reduction with sodium borohydride followed by formation of the phenylboronates indicated the addition of four molecules of phenylboronate to each toxin (Table III, part 3). Thus, PM toxin A must have four β-keto alcohol groups, and PM toxin B must have only three such groups plus a set of β-hydroxy alcohols. PM toxins C and D are similar to PM toxin B but with one extra secondary alcohol group as shown by the addition of a single Me_3Si ether linkage after reduction and phenylboronate ester formation (Table III, part 4).

These postulates were supported by mass spectra obtained by reducing PM toxins with $NaBD_4$ and then derivatizing with phenylboronic acid. The molecular ion of PM toxin B was four mass units higher (940), indicating four carbonyl groups,

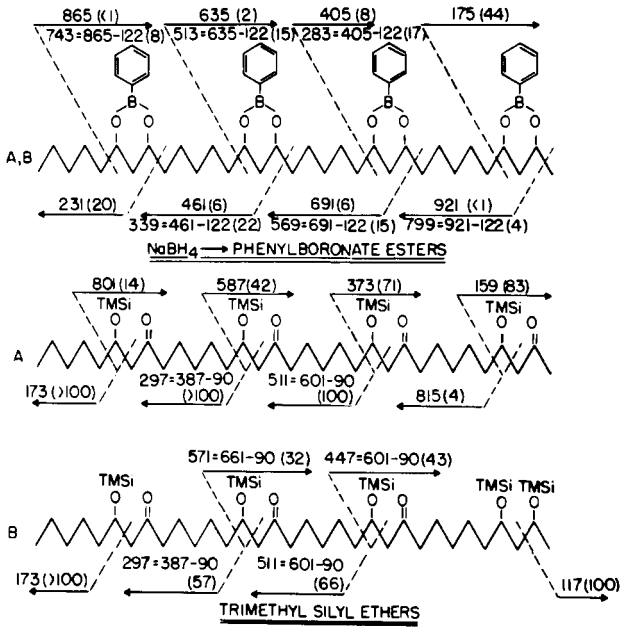

FIGURE 5: Patterns of EI-MS fragmentation of derivatives of PM toxins A and B. (Top scheme) Phenylboronate esters formed after reduction by $NaBH_4$. The patterns were the same for PM toxins A and B. (Lower schemes) Distinctive patterns for trimethylsilyl (TMSi) ethers of PM toxins A and B. Numbers in parentheses are ion intensities relative to the reference peaks given in Table III. Numbers followed by equal sign indicate observed fragments that arose from further loss of Me_3SiOH (m/z 90) or $C_6H_5B(OH)_2$ (m/z 122).

while PM toxins B and C were only three mass units higher (939 and 983, respectively) than the corresponding derivatives prepared from $NaBH_4$ (Table III).

Positions of β-Oxygen Functions. Signals at δ 0.84 and 14.1 in proton and ^{13}C NMR spectra, respectively, occur in all four PM toxin acetate derivatives (Figure 2) and correspond to chemical shifts assigned previously (Kono & Daly, 1979) to a methyl group terminating a chain of four methylene groups at the left side of the HMT toxin species as drawn in Figure 1. In addition, NMR spectra of PM toxins A and D show chemical shifts at δ 2.15 (proton) and 30.6 (^{13}C), which can be assigned (Kono & Daly, 1979) to a methyl ketone group at the other terminus of the underivatized molecules (Figure 1). However, PM toxins B and C acetates have absorptions at δ 1.22 (proton NMR) and 20.2 (^{13}C NMR), indicating a terminal methylcarbinol group for underivatized PM toxins B and C.

Analysis of the fragmentation patterns (Figures 5 and 6) of various derivatives supports these assignments. The patterns from the $(PhBO_2)_4$ esters of reduced PM toxins A and B were identical (Figure 5) and show an M^+ minus CH_3 peak, as well as an ion (m/z 175) corresponding to the loss of four terminal carbons carrying a phenylboronate ester group. Both PM toxin A tetrasilyl ether and toxin B pentasilyl ether exhibited an intense peak at m/z 173 (Figure 5). However, m/z 117 (C_2H_4O + Me_3Si) was a major peak only for toxin B, thus indicating that the two compounds differ only in reduction of a terminal methyl ketone in toxin A to a methylcarbinol in toxin B. Other diagnostic ions (Figure 5) indicated that the other β-oxygen functions are separated by bridges of five methylene groups.

The situation is more complex for PM toxins C and D, both of which have nine molecules of oxygen rather than eight. MS of the $(PhBO_2)_4$ Me_3Si, $PhBO_2$ $(Me_3Si)_4$, $(Me_3Si)_6$ derivatives of PM toxin C (Figure 6) all showed an intense peak at m/z 117, indicating a terminal methylcarbinol function. For PM toxin D Me_3Si derivatives, m/z 117 was not a diagnostic peak, but m/z 173 was. Other diagnostic masses from derivatives of both toxins C and D suggested that each toxin has a single set of three β-hydroxyl groups, located in a terminal chain of six carbon atoms shown on the left side for PM toxin C (Figure 6), but in a chain of ten carbon atoms shown on the right side in PM toxin D (Figure 6). If so, the following reaction should

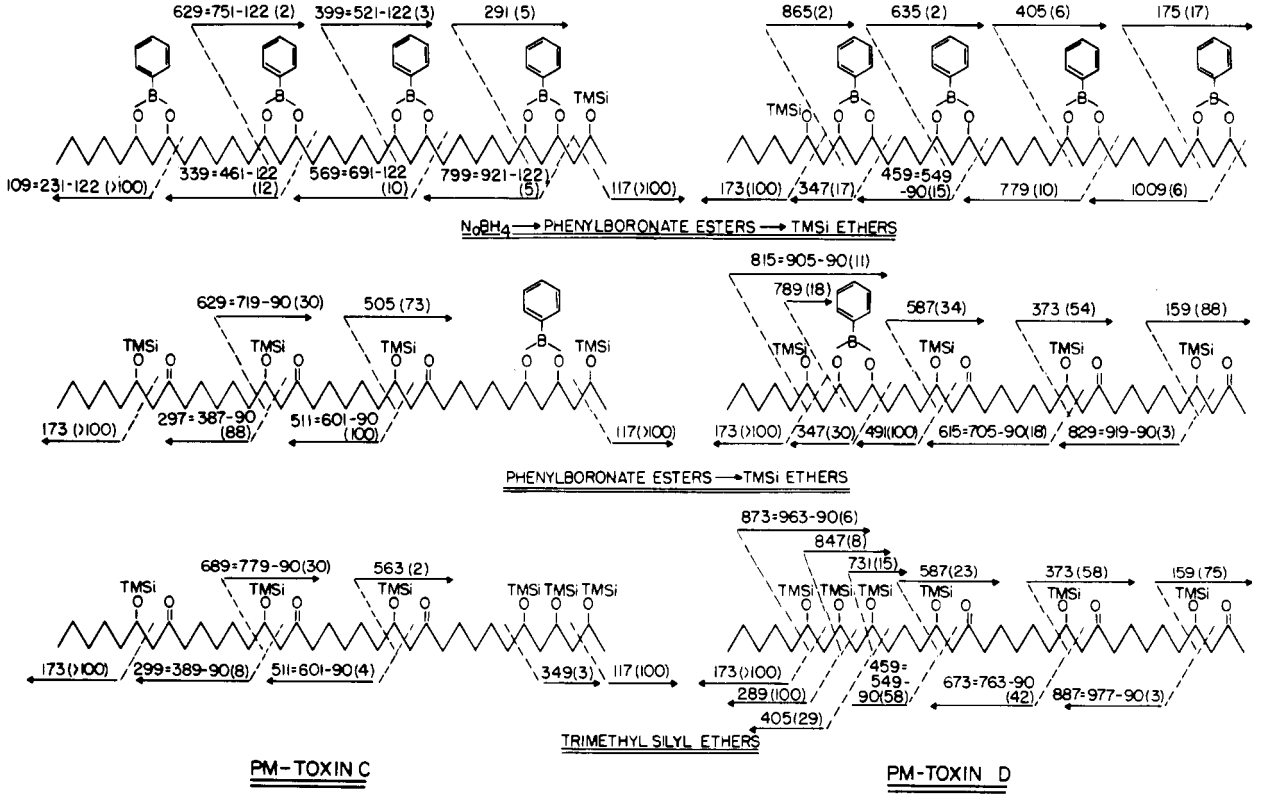

FIGURE 6: Patterns of EI-MS fragmentation of derivatives of PM toxins C and D. See legend of Figure 5 for details.

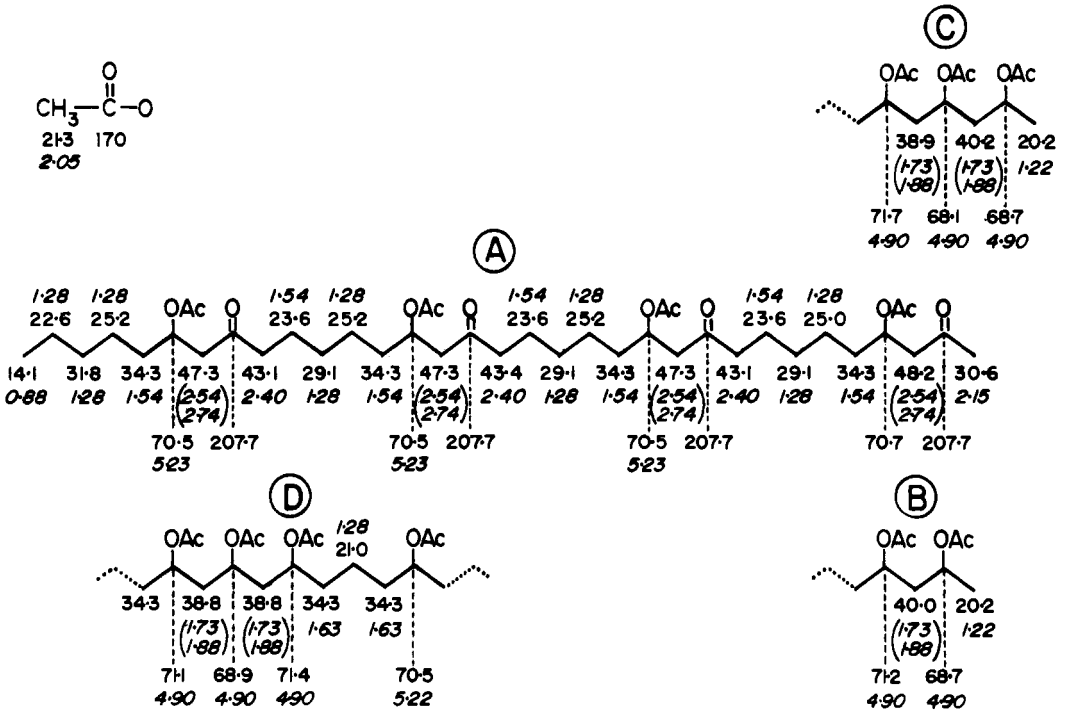

FIGURE 7: ^{13}C and ^{1}H (in italic) chemical-shift assignments obtained from 22.5- and 400-MHz NMR spectra and selective ^{1}H–^{13}C decoupling spectra of PM toxin acetate. Shifts given in parentheses show ABX-type coupling. Complete assignments are given for PM toxin A. Partial structures for PM toxins B–D show only portions of structures that are different than the assignments for PM toxin A.

Table IV: High-Resolution Mass Spectroscopy of PM Toxins B and C following Reduction and Formation of $(PhBO_2)_4$ Esters before Reaction with Trimethylchlorosilane

mass observed	assignment	deviation from theoretical (δ)
PM Toxin B		
936.62804 (M^+)	$C_{57}H_{80}O_8B_4$	2.4
569.3983 (691 − 122)[a]	$C_{36}H_{51}O_4B_2$	1.3
513.3333 (635 − 122)	$C_{32}H_{43}O_4B_2$	−2.9
339.2481 (461 − 122)	$C_{22}H_{32}O_2B$	−4.3
283.1867 (405 − 122)	$C_{18}H_{24}O_2B$	−0.9
231.1546 (231)	$C_{14}H_{20}O_2B$	−4.6
175.0932 (175)	$C_{10}H_{12}O_2B$	1.0
PM Toxin C		
1052.68836 (M^+)	$C_{62}H_{92}O_9SiB_4$	−3.7
936.62578	$C_{57}H_{80}O_8B_4$	3.3

[a] Numbers in parentheses indicate the possible origin of masses actually observed by loss of $C_6H_5B(OH)_2$ (m/z 122). See Figures 5 and 6.

Table V: High-Resolution Mass Spectroscopy of Trimethylsilyl Ethers of PM Toxins B and C

mass observed	assignment	deviation from expected (δ)
PM Toxin B		
856.58929 (M^+ − 90)[a]	$C_{45}H_{92}O_8Si_5$	−3.2
571.3708 (661 − 90)	$C_{29}H_{59}O_5Si_3$	4.0
511.3590 (601 − 90)	$C_{28}H_{55}O_4Si_2$	5.5
447.2820 (447)	$C_{21}H_{47}O_4Si_3$	4.0
297.2266 (387 − 90)	$C_{17}H_{33}O_2Si$	0.8
173.1354 (173)	$C_9H_{21}OSi$	−0.6
117.0729 (117)	$C_5H_{13}OSi$	0.5
PM Toxin C		
687.4313 (687)	$C_{34}H_{71}O_6Si_4$	−2.5
563.3447 (563)	$C_{26}H_{59}O_5Si_4$	1.3
511.3616 (601 − 90)	$C_{28}H_{55}O_4Si_2$	−4.8
473.2968 (563 − 90)	$C_{23}H_{49}O_4Si_3$	6.2
259.1555 (349 − 90)	$C_{12}H_{27}O_2Si_2$	2.2

[a] Numbers in parentheses indicate possible origin of observed mass by loss of Me_3SiOH (m/z 90).

be possible for the $PhBO_2$ or $(PhBO_2)_4$ Me_3Si ethers of PM toxin C, resulting in masses of 936 or 888, respectively:

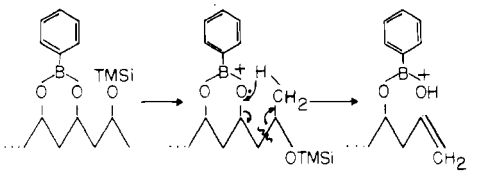

These masses are 22 and 15% of the base peak in the mass spectra of $(PhBO_2)_4$ Me_3Si ethers of PM toxin C but were not diagnostic for PM toxin D. Additional evidence stems from the fact that like PM toxin A or B, m/z 175 was a prominent ion in the spectrum of the $(PhBO_2)_4$ Me_3Si ether of PM toxin D but not in the spectrum of toxin C, suggesting that only two β-oxygen functions are present at one terminus of PM toxin D. Overall, the results (Figure 6) indicate that the β-oxygen functions in PM toxin C, as in PM toxins A and B, are separated by three methylene bridges of five carbons each. In PM toxin D, there are two such bridges plus one of only three methylene groups (Figure 6).

The assumptions about the chemical composition of ions observed in low-resolution MS are supported by high-resolution MS, in which the compositions of parent ions of the $(PhBO_2)_4$ esters of PM toxins B and C were determined by peak matching (Table IV). Other diagnostic ions are included, but only for toxin B $(PhBO_2)_4$ since they were identical with those of PM toxin C. As noted earlier, derivatives with Me_3Si ether linkages were less stable, but the composition of some of the more stable larger fragments were established (Table V).

NMR Assignments. Figure 7 summarizes all the ^{1}H and ^{13}C chemical shifts for PM toxin A tetraacetate obtained with 400- and 22.5-MHz spectra, respectively, in $CDCl_3$. Also shown as inserts are data for structural features that are characteristic of PM toxins B–D. All other chemical shift assignments for these compounds are common with those of

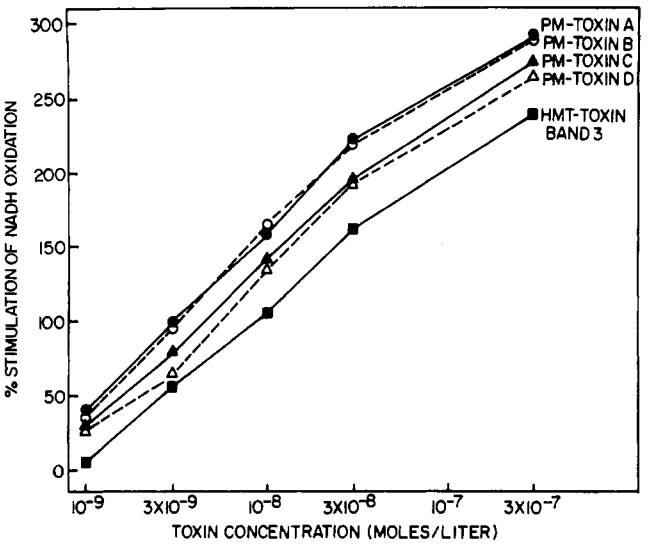

FIGURE 8: Comparisons of activity of PM toxins A–D with HMT toxin band 3 (see Figure 1) in stimulating NADH oxidation of mitochondria isolated from susceptible Tms corn. No effects on NADH oxidation were observed with mitochondria from resistant corn at approximately 10^{-5} M.

PM toxin A. The assignments, aided by ^{1}H–H decoupling, were verified by selective ^{13}C–{^{1}H} decoupling. Many of the methylene proton signals overlapped, and for these protons an approximate shift (δ 1.28 or 1.54) is given. The methylene groups between oxygenated carbon atoms exhibited ABX-type coupling, and thus two chemical shifts are assigned to them in parentheses. In ^{13}C spectra, CH–OAc assignments were made by comparison with HMT toxin (Kono & Daly, 1979). Some of these assignments, for example, the carbon nuclei of terminal β-alcohols of PM toxin C hexaacetate (δ 68.7 and 68.1), may be interchanged.

The assignment of a ^{13}C chemical shift of δ 21.0 to the central methyl carbon in the $-(CH_2)_3-$ bridge of PM toxin A (Figure 7) was possible through use of selective proton decoupling made with double pulses (180 or 90°) of ^{13}C NMR spectra. In this mode, interfering absorptions of the methyl carbon atoms of acetyl groups (δ 21.3) are observed as a quartet of negative peaks. Irradiation of the protons absorbing at δ 1.28 resulted in the enhancement of a positive peak at δ 21.0, as well as signals, as expected, at δ 25.2, 28.7, 34.3, and 38.8 (see Figure 7).

Effects on Mitochondria. Miller & Koeppe (1971) first demonstrated that mitochondria isolated from susceptible, but not from resistant, corn are affected by HMT toxin from *H. maydis*. NADH oxidation is stimulated (but malate oxidation is inhibited) within seconds (Payne et al., 1980b) at approximately 5×10^{-9} M (Suzuki et al., 1983). As with dark CO_2 fixation (Table I), the PM toxin complex consistently caused greater stimulation of NADH oxidation on a weight basis than HMT toxin (data not shown). Individual PM toxins also were consistently more active than isolated HMT toxin species on a molar basis (Figure 8) and were indistinguishable in activity from the native PM toxin complex on a weight basis. This suggests, as with HMT toxin (Payne et al., 1980a), that all components of the mixture probably are equally toxic. Although Figure 8 shows some small differences among PM toxins A–D, it has not been possible so far to establish statistically significant differences among them. PM toxin had no effects on NADH oxidation in mitochondria from resistant corn at concentrations 1000 times as great as those required to give 100% stimulation of state 4 rates of NADH oxidation in sensitive mitochondria from Texas male sterile plants.

At present, the biochemical site(s) of action for HMT toxin or PM toxin is (are) unkown. It has been suggested that HMT toxin may perturb membrane functions by altering inner mitochondrial membrane integrity (Matthews et al., 1979). An alternate suggestion is that it functions by binding to a polypeptide (M_r 13 000) of unknown function that has been demonstrated (Forde et al., 1978) to be synthesized in mitochondria of susceptible, but not resistant, corn. It also has been pointed out (Payne et al., 1980b; Daly, 1981) that the structural features of HMT toxin, particularly its chain length, might permit it to function as an ionophore. It recently has been reported in abstract form (Kimber & Sze, 1983) that Ca^{2+} transport is affected by HMT toxin in sensitive mitochondria only.

The biological activities (Suzuki et al., 1982b) observed with C_{15} to C_{26} synthetic analogues of HMT toxin (Suzuki et al., 1982a) also reinforce the importance of chain length for toxicity of HMT toxin. These shorter versions were less active than native HMT toxin or of its isolated components (Suzuki et al., 1982b). Recently, a C_{41} analogue has been synthesized and shown to have identical quantitative activity as native toxin or its components (Suzuki et al., 1983). Direct comparison of the C_{25} and C_{41} analogues revealed that the biological activity of a single molecule of the synthetic C_{41} was equivalent to that of 300 molecules of the C_{25} analogue (Suzuki et al., 1983).

The apparently greater activity of PM toxins (Figure 8), with chain lengths of only 33 or 35 carbons, therefore was somewhat unexpected. However, when space-filling molecular models of HMT and PM toxins are compared, it is intriguing that the spacing of the four sets of oxygen functions is nearly identical, as indicated two dimensionally in Figures 1 and 2 and three dimensionally in the construction of space-filling models. Whether such spacing is involved with action as an ionophore or in binding to, or insertion into, a specific site is under investigation. Determination of a mode of action of these interesting compounds may be facilitated by the use of PM toxins, rather than HMT toxins, because their structures are less complicated. A comparative study of the biosynthetic pathways of these compounds also would be of interest.

Acknowledgments

We thank Y. Esumi, Institute of Physical and Chemical Research, for field-desorption and high-resolution mass spectra and the Midwest Center for Mass Spectrometry, a National Science Foundation Regional Instrumentation Facility (Grant CHE8211164), for fast-atom bombardment and high-resolution mass spectra.

Registry No. PM toxin A, 88212-12-8; PM toxin B, 87879-56-9; PM toxin C, 87879-55-8; PM toxin D, 88212-13-9.

References

Comstock, J. C., Martinson, C. A., & Gengenbach, B. G. (1973) *Phytopathology 63*, 1357–1361.

Cope, A. C., Bly, R. K., Burrows, E. P., Ceder, O. J., Ciganek, E., Gillis, B. T., Porter, R. F., & Johnson, H. E. (1962) *J. Am. Chem. Soc. 84*, 2170–2178.

Daly, J. M. (1981) in *Toxins in Plant Disease* (Durbin, R. D., Ed.) pp 331–394, Academic Press, New York.

Daly, J. M., & Barna, B. (1980) *Plant Physiol. 66*, 580–583.

Daly, J. M., Kono, Y., Suzuki, Y., & Knoche, H. W. (1983) in *Pesticide Chemistry. Human Welfare and the Environment* (Miyamoto, J., & Kearney, P. C., Eds.) Vol. II, pp 11–20, Pergamon Press, Oxford.

Forde, B. G., Oliver, R. J. C., & Leaver, C. J. (1978) *Proc. Natl. Acad. Sci. U.S.A. 75*, 3841–3845.

Kimber, A., & Sze, H. (1983) *Plant Physiol. 72 (Suppl.)*, 161.
Koeppe, D. E., Cox, J. K., & Malone, C. P. (1978) *Science (Washington, D.C.) 201*, 1227-1229.
Kono, Y., & Daly, J. M. (1979) *Bioorg. Chem. 8*, 391-397.
Kono, Y., Takeuchi, S., Kawarada, A., Daly, J. M., & Knoche, H. W. (1980) *Tetrahedron Lett. 21*, 1537-1540.
Kono, Y., Knoche, H. W., & Daly, J. M. (1981) in *Toxins in Plant Disease* (Durbin, R. D., Ed.) pp 221-257, Academic Press, New York.
Leaver, C. J., & Gray, M. W. (1982) *Annu. Rev. Plant Physiol. 33*, 373-402.
Matthews, D. E., Gregory, P., & Gracen, V. E. (1979) *Plant Physiol. 63*, 1149-1153.
Miller, R. J., & Koeppe, D. E. (1971) *Science (Washington, D.C.) 173*, 67-69.
Payne, G., Knoche, H. W., Kono, Y., & Daly, J. M. (1980a) *Physiol. Plant Pathol. 16*, 227-239.
Payne, G., Kono, Y., & Daly, J. M. (1980b) *Plant Physiol. 65*, 785-791.
Pringle, R. B., & Scheffer, R. P. (1963) *Phytopathology 53*, 785-787.
Suzuki, Y., Knoche, H. W., & Daly, J. M. (1982a) *Bioorg. Chem. 11*, 300-312.
Suzuki, Y., Tegtmeier, K. J., Daly, J. M., & Knoche, H. W. (1982b) *Bioorg. Chem. 11*, 313-321.
Suzuki, Y., Danko, S. J., Daly, J. M., Kono, Y., Knoche, H. W., & Takeuchi, S. (1983) *Plant Physiol. 73*, 440-444.
Tegtmeier, K. J., Daly, J. M., & Yoder, O. C. (1982) *Phytopathology 72*, 1492-1495.
Yoder, O. C. (1973) *Phytopathology 63*, 1361-1366.

Synthesis and Biological Activity of 5′-Capped Derivatives of 5′-Triphosphoadenylyl(2′→5′)adenylyl(2′→5′)adenosine†

Jiro Imai and Paul F. Torrence*

ABSTRACT: The oligonucleotides A5′pp5′A2′p5′A2′p5′A and A5′ppp5′A2′p5′A2′p5′A were prepared by reaction of AMP or ADP, respectively, with the 5′-(phosphoimidazolidate) of A2′p5′A2′p5′A. A5′pppp5′A2′(p5′A)$_n$ (n = 1-3) were synthesized by reaction of p5′A2′(p5′A)$_n$ (n = 1-3) with adenosine 5′-trimetaphosphate. All structures were confirmed by enzyme digestion and ^{1}H and ^{31}P nuclear magnetic resonance (NMR). The products A5′pppp5′A2′p5′A and A5′pppp5′A2′p5′A2′p5′A were found to be identical with two of the products of the 2-5A synthetase catalyzed reaction of Ap_4A with ATP, thus confirming the structural assignments made by earlier investigators. In extracts of mouse L cells programmed with encephalomyocarditis virus RNA, A5′pppp5′A2′p5′A2′p5′A2′p5′A and A5′pppp5′A2′p5′A2′p5′A were equipotent with 2-5A itself as inhibitors of translation. The oligomers A5′ppp5′A2′p5′A2′p5′A and A2′pppp5′A2′p5′A were about 100 times less active than 2-5A, and A5′pp5′A2′p5′A2′p5′A was without translational inhibitory activity. When affinity for the 2-5A-dependent endonuclease was determined (by displacement of 2-5A[^{32}P]pCp from endonuclease), all of the analogues, as well as 2-5A itself, had similar affinities for the endonuclease except for A5′pppp5′A2′p5′A, which was bound ~100 times less effectively. Under conditions of the radiobinding assay, A5′pppp5′A2′p5′A2′p5′A was degraded ($t_{1/2}$ = 2 h) to ATP, ADP, AMP, ppp5′A2′p5′A2′p5′A, and p5′A2′p5′A2′p5′A. The same products were obtained when degradation was carried out under protein synthesis conditions at 30 °C except that the half-life of A5′pppp5′A2′p5′A2′p5′A was reduced to 3 min. The other unsymmetrical di- and triphosphates A5′pp5′A2′p5′A2′p5′A and A5′ppp5′A2′p5′A2′p5′A were degraded much more slowly than the tetraphosphate, and they did not give rise to 2-5A as a degradation product. When the degradation of A5′pppp5′A2′p5′A2′p5′A was examined in incubation mixtures containing human serum or Nalmalwa cell extract, it was found that the tetraphosphate was quite stable to the action of human serum but was readily degraded to 2-5A and p5′A2′p5′A2′p5′A by extracts of the human lymphoblastoid cells. Thus, "capping" (with adenosine) of the β- or γ-phosphates of the established translational inhibitors pp5′A2′p5′A2′p5′A or ppp5′A2′p5′A2′p5′A led to a loss of ability to activate the 2-5A-dependent endonuclease even though such oligomers still were bound to the endonuclease as well as 2-5A itself. However, capping with an adenosine tetraphosphate moiety gave a 2-5A derivative that was stable in the external milieu of the cell but that was rapidly cleaved by the enzyme(s) of the cytosol to give 2-5A itself.

The established role of 2-5A[1] (Kerr & Brown, 1978) in the antiviral action of interferon [for reviews see Torrence (1982), Lengyel (1982), and Sen (1982)], its possible role (Kimchi et al., 1981a,b) in interferon's antiproliferative action (Gresser & Tovey, 1978; Taylor-Papadimitriou, 1980), and its possible involvement in regulation of cell growth, differentiation, and/or development (Stark et al., 1979; Etienne-Smekens et al., 1983a,b; Krishnan & Baglioni, 1980; Oikarinen, 1982; Besancon et al., 1981; Kimchi, 1981) have resulted in interest in the 2-5A system as a new approach to antiviral and/or antitumor agents. Two problems associated with envisaged application of the 2-5A system have been defined (Torrence et al., 1982) to include the relative lability of 2-5A toward degrading enzymes and the cellular impermeability of the highly charged 2-5A molecule. While a solution of the first problem has been provided by chemical modification of the 2-5A molecule to yield analogues resistant to degradation

† From the Laboratory of Chemistry, National Institute of Arthritis, Diabetes, Digestive and Kidney Diseases, National Institutes of Health, Bethesda, Maryland 20205. *Received June 7, 1983.*

[1] Abbreviations: 2-5A, pppA2′p(A2′p)$_n$A where n = 1 to about 10; TEAB, triethylammonium bicarbonate; Im(pA)$_3$, 5′-imidazolidate of p5′A2′p5′A2′p5′A; NMR, nuclear resonance; EDTA, ethylenediaminetetraacetic acid; Tris, tris(hydroxymethyl)aminomethane.

0006-2960/84/0423-0766$01.50/0